Online Analysis of Single Cyanobacteria and Algae Cells under Nitrogen-Limited Conditions Using Aerosol Time-of-Flight Mass Spectrometry

ARTICLE *in* ANALYTICAL CHEMISTRY · AUGUST 2015

Impact Factor: 5.64 · DOI: 10.1021/acs.analchem.5b02326 · Source: PubMed

7 AUTHORS, INCLUDING:

Nathan Schoepp

California Institute of Technology

8 PUBLICATIONS **116** CITATIONS

SEE PROFILE

Joris Beld

Drexel University College of Medicine

20 PUBLICATIONS **503** CITATIONS

SEE PROFILE

Michael D Burkart

University of California, San Diego

140 PUBLICATIONS **3,213** CITATIONS

SEE PROFILE

Kim Prather

University of California, San Diego

295 PUBLICATIONS **9,796** CITATIONS

SEE PROFILE

analytical chemistry

Editors' Highlight

pubs.acs.org/ac

Online Analysis of Single Cyanobacteria and Algae Cells under Nitrogen-Limited Conditions Using Aerosol Time-of-Flight Mass Spectrometry

John F. Cahill,[‡,∥] Thomas K. Darlington,[†] Christine Fitzgerald,[†] Nathan G. Schoepp,[‡,⊥] Joris Beld,[‡] Michael D. Burkart,[‡] and Kimberly A. Prather*[,‡,§]

[†]nanoComposix, San Diego, California 92111, United States

[‡]Department of Chemistry and Biochemistry, University of California, La Jolla, California 92093, United States

[§]Scripps Institution of Oceanography, University of California, La Jolla, California 92093, United States

Supporting Information

ABSTRACT: Metabolomics studies typically perform measurements on populations of whole cells which provide the average representation of a collection of many cells. However, key mechanistic information can be lost using this approach. Investigating chemistry at the single cell level yields a more accurate representation of the diversity of populations within a cell sample; however, this approach has many analytical challenges. In this study, an aerosol time-of-flight mass spectrometer (ATOFMS) was used for rapid analysis of single algae and cyanobacteria cells with diameters ranging from 1 to 8 μm. Cells were aerosolized by nebulization and directly transmitted into the ATOFMS. Whole cells were determined to remain intact inside the instrument through a combination of particle sizing and imaging measurements. Differences in cell populations were observed after perturbing *Chlamydomonas reinhardtii* cells via nitrogen deprivation. Thousands of single cells were measured over a period of 4 days for nitrogen-replete and nitrogen-limited conditions. A comparison of the single cell mass spectra of the cells sampled under the two conditions revealed an increase in the dipalmitic acid sulfolipid sulfoquinovosyldiacylglycerol (SQDG), a chloroplast membrane lipid, under nitrogen-limited conditions. Single cell peak intensity distributions demonstrate the ability of the ATOFMS to measure metabolic differences of single cells. The ATOFMS provides an unprecedented maximum throughput of 50 Hz, enabling the rapid online measurement of thousands of single cell mass spectra.

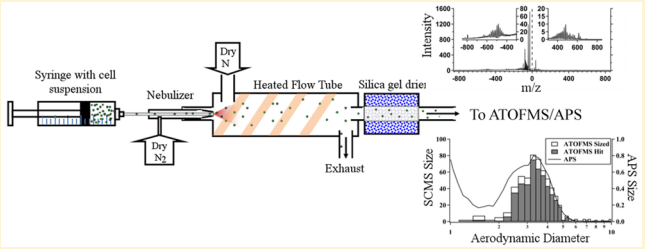

Most metabolomics studies typically use measurements of cell populations to elucidate aggregate cell behavior and functions; however, the behavior of any one cell cannot be determined from bulk averages. Cell analysis has consistently progressed to finer resolution, with an increasing focus on single cells.[1−4] Cell populations are inherently heterogeneous; each cell may differ due to its history, microenvironment, age, health, and genetics. Analysis with single cell resolution has the potential to provide insight into complicated and dynamic metabolic interactions between cells.

Single cell analysis presents a significant analytical challenge. Analyte concentrations are low and high throughput is needed to obtain enough data to statistically distinguish differences in cell populations or subpopulations. Many techniques have emerged to provide single cell measurements including capillary electrophoresis,[5−13] fluorescence[8,14−16] electrospray ionization mass spectrometry,[13,17−20] and matrix-assisted laser desorption ionization mass spectrometry (MALDI-MS).[14,21−25] For more information on these techniques and the state of single cell analysis, the reader is referred to numerous reviews on the subject.[1−4,26−31]

Mass spectrometry (MS) techniques have the highest potential for single cell analysis as these techniques have the potential for both high sensitivity and throughput; however, most existing MS techniques are limited by their throughput. The Zenobi group has made great progress in single cell analysis using the microarrays for mass spectrometry (MAMs) platform, which deposits single cells into individual microarrays for subsequent analysis by MALDI-MS.[21,24,32] The MAMs platform has reported a throughput of 2 Hz, which is significantly greater than most other single-cell techniques.[32] It has also demonstrated the power of single cell metabolomics by distinguishing differences in cell populations of yeast undergoing various stimuli and by providing mechanistic information on these processes.[24]

Aerosol time-of-flight mass spectrometry (ATOFMS), primarily used for measuring atmospheric aerosol composition,[33] and most recently for characterization of nanoparticle materials,[34,35] can measure single aerosol particles in real-time.

Received: June 19, 2015
Accepted: August 3, 2015
Published: August 3, 2015

DOI: 10.1021/acs.analchem.5b02326
Anal. Chem. 2015, 87, 8039−8046

Table 1. Description and Sizing Analysis of the Cells Tested in the ATOFMS

genus/species	type	acronym	ATOFMS size (μm)	APS size (μm)	size % error
Chlamydomonas reinhardtii	freshwater microalgae	*Cr*	3.1	3.3	6%
Scenedesmus dimorphus	freshwater microalgae	*Sd*	3.7	4.1	10%
Dunaliella tertiolecta	marine microalgae	*Dt*	3.1	2.9	7%
Nannochloropsis salina	marine microalgae	*Ns*	2.1	2	5%
Porphyridium purpera	marine microalgae	*Pp*	4.6	4.4	5%
Chlorella vulgaris	freshwater microalgae	*Cv*	3.1	2.1	48%
Anabaena sp. PCC 7120	freshwater cyanobacteria	*Asp*	3.2	3.3	3%
Synechococcus elongatus	freshwater cyanobacteria	*Se*	1.5	1.1	36%

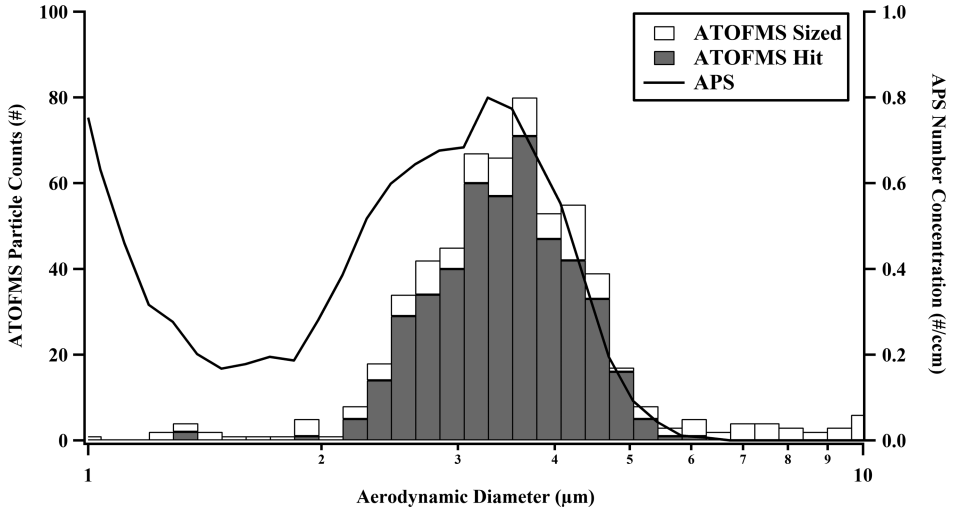

Figure 1. Comparison of APS and ATOFMS sizing measurements of *Chlamydomonas reinhardtii*. Cells sized by ATOFMS are given in white bars, and those cells that also generated mass spectra are shown in the filled bars.

When analyzing individual aerosol particles, this technique requires no sample preparation, can probe aerosol particles rapidly (as fast as 50 Hz depending on the ionization laser used), is highly sensitive (down to zeptomoles of specific analytes),[36] and collects dual polarity mass spectra and size of each particle. These features together distinguish ATOFMS from other techniques being used in single cell analysis by enabling rapid analysis of thousands of individual cells in a relatively short time, provided that cells can be aerosolized and transmitted into the instrument.

Herein an ATOFMS is used for rapid analysis of single cells with aerodynamic diameters ranging from 1 to 10 μm. Using a combination of imaging and sizing measurements, whole cells were verified to be transmitted intact within the ATOFMS. Thousands of single algae and cyanobacteria cells were rapidly aerosolized and analyzed using ATOFMS, demonstrating the wide applicability and high throughput nature of this technique. Changes in single cell metabolite distributions were observed in the model alga *Chlamydomonas reinhardtii* under nutrient deprivation for both "bulk" and single cell measurements.

EXPERIMENTAL SECTION

Cell Preparation. The algal and cyanobacteria strains used to characterize the capabilities of the ATOFMS for single cell analysis are summarized in Table 1 and include *Chlamydomonas reinhardtii* (*Cr*), *Chlorella vulgaris* (*Cv*), *Dunaliella tertiolecta* (*Dt*), *Scenedesmus dimorphus* (*Sd*), *Porphyridium purpureum* (*Pp*), *Anabaena* sp. PCC 7120 (*Asp*), *Nannochloropsis salina* (*Ns*), and *Synechococcus elongatus* (*Se*). The *Cr* strain was obtained from the Chlamydomonas Resource Center. Their preparation is discussed in the Supporting Information. It should be stressed that no additional fixatives or epoxies were added to the cells before analysis, reducing complications in the interpretation of the mass spectra.

For experiments involving *Cr* nutrient deprivation, cell counts and autofluorescence were taken daily. Samples were transesterified in situ in 0.5 mL of 1 M HCl/MeOH for 1 h prior to being extracted twice with hexanes for analysis by GC/MS. Hexanes were evaporated and the fatty acid methyl esters resuspended in 1.25 mL of hexane. The lipid content in a cell sample is estimated by the sum of the peak areas observed by GC/MS. Three separate trials were conducted. Cell response was found to vary trial to trial, indicating cell culture variability for *Cr* and thus each trial necessitated independent characterization. For clarity, only trial 1 is discussed in the main text. A full description of trials 2 and 3 is given in the Supporting Information.

Aerosol Time-of-Flight Mass Spectrometry. The ATOFMS is equipped with a newly developed particle aerodynamic lens for transmission of larger aerosol particles and whole cells with diameters between 1 and 10 μm.[37,38] The aerodynamic lens is a critical feature of the ATOFMS used in this study, as whole cells of eukaryotes are typically >2 μm in diameter. After cells have been aerosolized, they enter the instrument and are focused into a collimated beam by the aerodynamic lens. The cells then enter a particle sizing region where they pass through two continuous wave lasers spaced 6 cm apart. The difference in time between scattering signals produced by each laser is used to determine the velocity of the cell within the instrument. After calibration with polystyrene

DOI: 10.1021/acs.analchem.5b02326
Anal. Chem. 2015, 87, 8039−8046

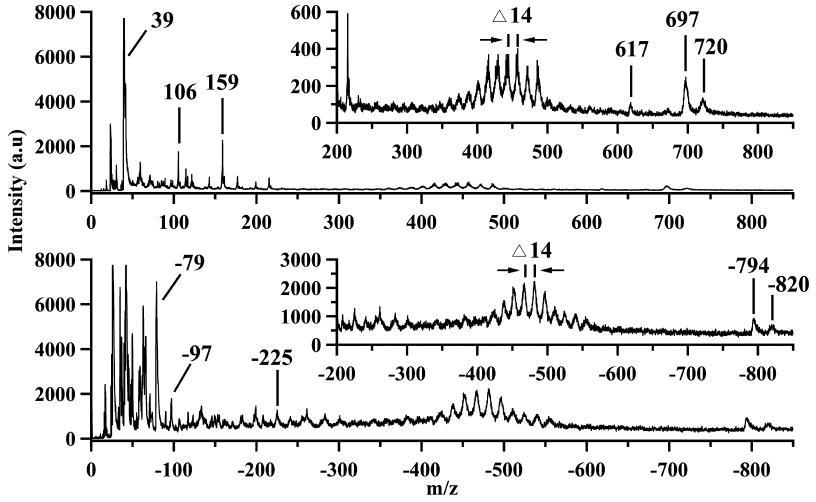

Figure 2. Representative positive (top) and negative (bottom) ion mass spectra of a single *Chlamydomonas reinhardtii* cell. The insets highlight the higher m/z peaks.

latex spheres (PSLs) of known size, the velocity can be converted into the aerodynamic diameter. The velocity also synchronizes the firing of a 266 nm Nd:YAG laser (Quantel) for desorption and ionization of each sized cell. The resulting ions are collected using a dual polarity Z-configuration time-of-flight mass spectrometer.[37] Thus, for each individual cell, both size and dual polarity mass spectra are acquired. The ATOFMS is capable of acquiring data at rates as high as 50 Hz, limited by the repetition rate of the desorption/ionization laser. This, in combination of the range of chemical data acquired using mass spectrometry, makes the ATOFMS ideal for single cell analysis.

Mass spectrometry data were imported into Matlab (Matlab, Inc.) using the YAADA[39] toolkit (www.yaada.org) and was filtered to select only whole cell distributions by using a combination of size and peak height distributions (Figures S-1 and S-2). This process is discussed in more detail in the Supporting Information.

Cell Aerosolization. A syringe containing cell solution was pumped at 0.1 mL min^{-1} into a C-type concentric nebulizer (Precision Glassblowing, CO) and nebulized using dry nitrogen at 35 psi. The experimental setup is shown in the Supporting Information Figure S-3. After nebulization, the aerosol passes through a heated flow tube and diffusion dryer, which removes any water present. The output is then sent to an aerodynamic particle sizer (APS) and the ATOFMS in parallel. The APS and ATOFMS both measure the particle aerodynamic diameter making the two techniques directly comparable. Other nebulizers and aerosolization methods were tried, such as a collison atomizer, but the C-type nebulizer yielded the highest whole cell number concentrations by APS, with minimal fragmentation. An externally mounted stir plate and a stir bar located within the syringe prevented agglomeration and cell settling during experiments.

RESULTS AND DISCUSSION

Verification of Whole Cell Transmission. The APS size histogram of *Chlamydomonas reinhardtii* (*Cr*) cells is shown in Figure 1. The mode of the size distribution peaks at 3.3 μm and is comparable to cell sizes measured via light microscopy before aerosolization. Additionally, for comparison, aerosol particles were deposited on a glass slide after aerosolization and drying. Imaging of this slide using dark field and fluorescent microscopy indicated that whole cells are present as well as cell fragments. Ideally, we would like to avoid cell fragmentation, but it is important to note that it does not limit the information content by ATOFMS. The ATOFMS measures the size of the cells in addition to individual cell mass spectra; hence, cell fragments (having smaller diameters than whole cells) can be identified, allowing the chemical investigation of only whole cells.

The ATOFMS-measured size distribution of *Cr* cells, also shown in Figure 1, has excellent agreement with APS measurements. The hit fraction (solid bars), representing those sized particles that also generated mass spectra, also match the APS size distribution, indicating transmission of intact whole cells throughout the ATOFMS, despite the high vacuum of the instrument. The vacuum susceptibility of cells is discussed in more detail in the Supporting Information. For complete validation, images of particle deposition slides in the particle sizing region of the instrument (Figure S-4) provide conclusive evidence that intact whole cells are being transmitted through the ATOFMS and that the measured sizes are accurate.

Single Cell Mass Spectra of Algae and Cyanobacteria Cells. Representative positive and negative mass spectra obtained from a single *Cr* cell are shown in Figure 2. To the best of the authors' knowledge, this is the first time an online single particle mass spectrometry technique has been used for the analysis of algae or eukaryotic cells. The *Cr* mass spectra show a broad range of information, with the mass/charge (m/z) as high as −820 in the negative ion mode. The identities of the majority of these peaks are unknown at this time, but a brief discussion of the peaks of interest is given here and in the Supporting Information. In the lower mass range (<200 m/z), there is evidence of metals ($^{23}Na^+$ and $^{40}Ca^+$) and organic fragment ions ($^{12}C^+$, $^{15}CH_3^+$, $^{59}NC_3H_9^+$) in the positive ion mode and $^{26}CN^-$, $^{42}CNO^-$, and $^{79}PO^{3-}$ ions in the negative ion mode. A broad range of peaks from m/z 143−215, 350−550, and additional peaks at m/z 617, 670, 696, and 720 can be seen in the positive ion mode. The cluster peaks between m/z 350−550 are separated by m/z 14, which also appear in the negative ion mode and are probably the result of fragmentation from fatty acids. Additional peaks at m/z −794 and −820 present in *Cr* cells are discussed later in the manuscript.

DOI: 10.1021/acs.analchem.5b02326
Anal. Chem. 2015, 87, 8039−8046

To demonstrate the wide applicability of the technique for the analysis of a broad range of cell types and cell sizes with relative ease, various cell strains were aerosolized and laser ablated in the ATOFMS. The cell name, type, their weighted average APS, and ATOFMS particle sizes are given in Table 1. The cells include algae and cyanobacteria species originating from freshwater or marine environments and exemplify the variety and sizes of cells that can be introduced into this system. As can be seen in Table 1, APS and ATOFMS measured cell diameters were in excellent agreement with sizing errors typically <10% indicating that single cells were being successfully transmitted through the instrument intact. Differences usually arose when cells were on the smaller end (<3 μm) of the ATOFMS size range where the inlet transmission efficiency is the lowest. It is also possible, though less likely, that these small cells fragmented once inside the high vacuum of the ATOFMS (~10^{-7} Torr), creating the discrepancy between APS size distributions which are collected near atmospheric pressure. A single cell mass spectrum for each cell type is given in Figure S-6. Spectra contained similarities between cell types (e.g., potential fragmentation of fatty acids between m/z 350−550) as well as unique features between cell types (e.g., small m/z relative intensities and ions >600 m/z). For these experiments, cells were acquired at a rate of ~1−3 Hz, as a concentrated cell solution was not used. Notably, thousands of single cell mass spectra could still be acquired over a short period of time (~1 h), and for each strain, minimal sample preparation was necessary (see the Supporting Information).

Nutrient Deprivation of Chlamymondas reinheirtii. An issue with any MS technique is its destructive nature and thus separating measurement variability (for which an average cannot be acquired) from cell-to-cell heterogeneity represents a major challenge. This problem was overcome by Ibanez et al. by stimulating a known metabolic change in *Saccharomyces cerevisiae* cells and monitoring the change in lipid content by mass spectrometry at both the "bulk" and single cell level.[24] Employing the same concept, *Cr* cells were deprived of nitrogen to induce the production of triacylglycerides (TAGs), lipid droplets, and other fatty acid comprised lipids.[40−44] Additionally, cells swell in size in response to nitrogen deprivation, which can be measured by the ATOFMS. Cells were monitored by ATOFMS over 4 days of nitrogen deprivation. Comparison of data at the bulk and single cell level can be used to determine if true differences are present between cell subpopulations.

Cell Growth and Size Distributions. Cell counts as a function of day for nitrogen-replete and nitrogen-limited conditions are given in Figure S-7 for trial 1. Cell solution color was monitored visually over the course of the experiment for nitrogen-limited conditions becoming light brown in color by day 4 while the color of nitrogen-replete samples remained a vibrant green throughout the experiment.

APS and ATOFMS measured size distributions under nitrogen-replete conditions for day 1 and day 4 are shown in Figure 3. Cell diameters peaked between 4 and 5 μm for each day of the experiment. This is consistent with measurements by microscopy before aerosolization. In contrast, cells under nitrogen-limited conditions nearly doubled in size over the course of the experiment, growing from 4−5 μm to 7−8 μm in aerodynamic diameter (Figure 3). This is due to the accumulation of various lipids under nitrogen-limited conditions.[40−44] Small particle noise generated during nebulization creates the APS mode for particles <3 μm. The ATOFMS does not transmit these particles effectively and thus differs from APS measurements in this size range. APS and ATOFMS size distributions for trials 2 and 3 were similar to trial 1 (Figure S-8).

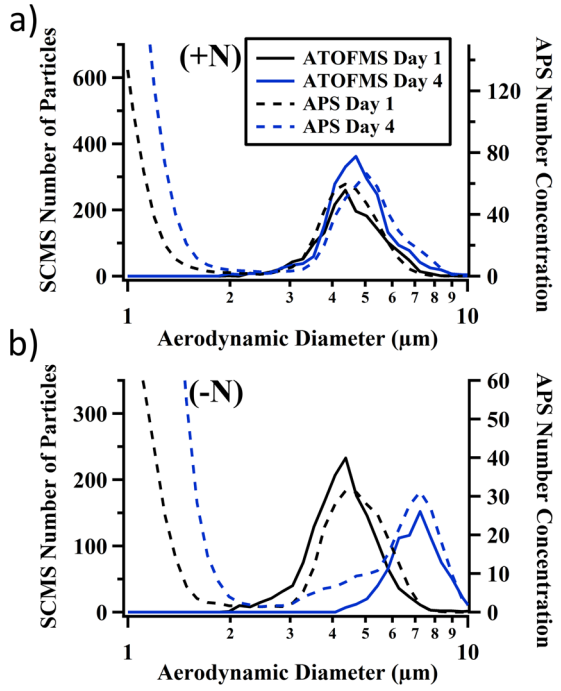

Figure 3. APS (dashed) and ATOFMS (solid) size distributions for day 1 (black) and day 4 (blue) of *Chlamydomonas reinhardtii* cells under nitrogen-replete (a) and nitrogen-limited (b) conditions.

Single Cell Mass Spectra under Nitrogen-Replete and Nitrogen-Limited Conditions. Average mass spectra for day 4 of trial 1 for nitrogen-replete and nitrogen-limited conditions are shown in Figures S-9 and S-10, respectively. Of interest is the fatty acid fragmentation profile that appears in the high m/z range in the positive and negative ion mass spectra. A difference mass spectrum, calculated as the difference between the average mass spectra from day 4 to day 1, highlights the major changes in composition over the course of the nitrogen deprivation experiment (Figure 4).

In the positive ion mass spectra, the nitrogen-replete and nitrogen-limited conditions exhibited similar differences over time. Ions <200 m/z were generally more intense at the beginning of the experiment while higher m/z ions (>200) increased in intensity. Peaks at m/z 617 and 696 showed a greater positive difference in nitrogen-limited samples. Across all trials these peaks, along with the fatty acid fragment ions (350−550 m/z), consistently increased in height under both conditions. Interestingly, nitrogen-replete samples differed considerably for trials 2 and 3. In trial 2, essentially no change was observed for ions >200 m/z (Figure S-13), whereas in Trial 3 (Figure S-16) all high mass ions decreased in intensity as the days progressed. Smaller m/z ions always decreased regardless of the sample condition.

The negative ion difference mass spectra (Figure 4) showed more variability than the positive ions. Smaller m/z ions are typically lower in intensity for either growth condition. Peaks attributed to fatty acid fragmentation (m/z 423−554) responded differently in every trial (Figures S-13 and S-16). Most striking in these spectra is the ion at m/z 794 which increases in intensity significantly only under nitrogen-limited

DOI: 10.1021/acs.analchem.5b02326
Anal. Chem. 2015, 87, 8039−8046

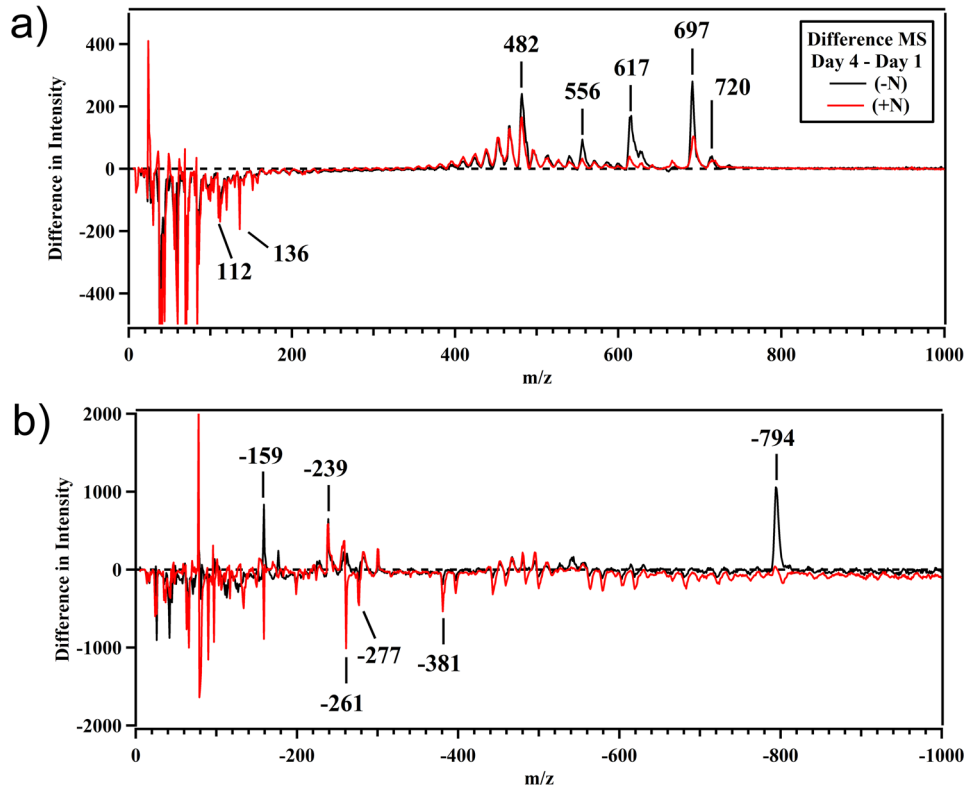

Figure 4. Positive and negative ion difference mass spectra (day 4 to day 1) of *Chlamydomonas reinhardtii* cells for nitrogen-replete (red) nitrogen-limited conditions (black) in trial 1.

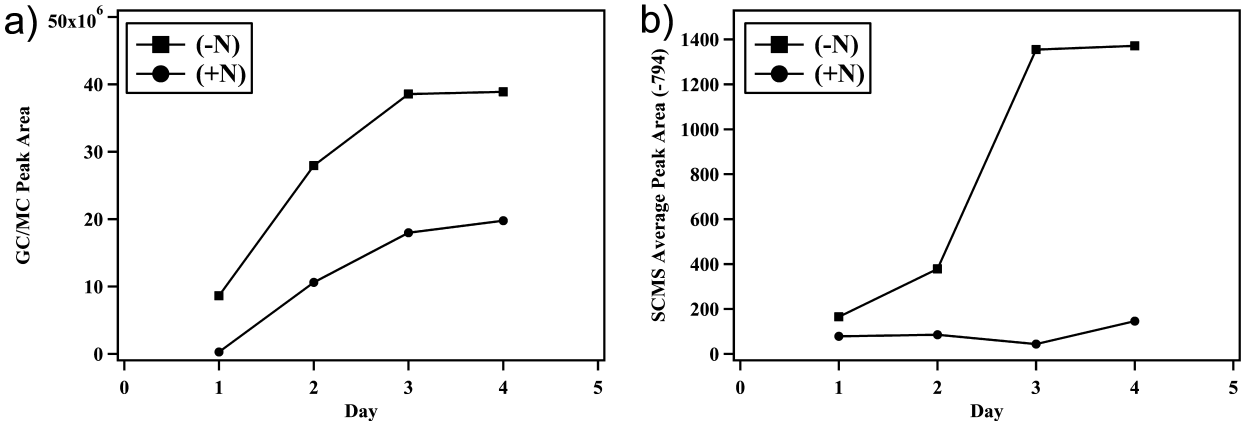

Figure 5. (a) Ensemble measurement of GC/MS 16:0 fatty acid peak area and (b) ATOFMS average peak area of 794 from thousands of single cell measurements of *Chlamydomonas reinhardtii* cells under nitrogen-replete (circles) and nitrogen-limited (squares) conditions.

conditions. This difference appears in every trial and is the most noteworthy feature differentiating nitrogen-replete from nitrogen-limited sample conditions. On the basis of separate ESI MS/MS measurements of a bulk sample, this peak is assigned to the lipid dipalmitic acid sulfoquinovosyldiacylglycerol (SQDG) (see the Supporting Information)

SQDG is one of the four common chloroplast membrane lipids along with mono- and digalatosyldiacylglycerol (MGDG and DGDG) and phosphoglycerol (PG). SQDG has been studied for its potential role in photosynthetic membranes and pigment−protein complexes; however, conflicting reports on the effects of N-limitation on SQDG levels in *Cr* cells exist.[45] Siaut et al. measured a significant decrease in SQDG and other membrane lipids, by ∼80%, with N-limitation.[46] In contrast, Sugimoto et al. found no degradation during N-limitation but did see an decrease in SQDG with sulfur-limitation.[47] Riekhof et al. found that phosphate-limitation resulted in a doubling of SQDG in wild-type cells.[48] In contrast, the data here indicate an increase in the dipalmitic acid SQDG with nitrogen-limitation.

Bulk GC/MS and ATOFMS SQDG Profiles. A quantitative measure of the 16:0 (carbon atoms:double bonds) fatty acid content in the cell samples can be measured using GC/MS. Figure 5a shows the results for nitrogen-replete and nitrogen-limited conditions. Interestingly total peak areas increase over time for both conditions, though the nitrogen-limited condition clearly generates more fatty acids over the course of the trial. In the nitrogen-replete condition, fatty acid content increased but less than in the nitrogen-limited case; however, the GC/MS data varied considerably between trials (Figures S-11 and S-14). The nitrogen-limited conditions consistently generated higher

DOI: 10.1021/acs.analchem.5b02326
Anal. Chem. 2015, 87, 8039−8046

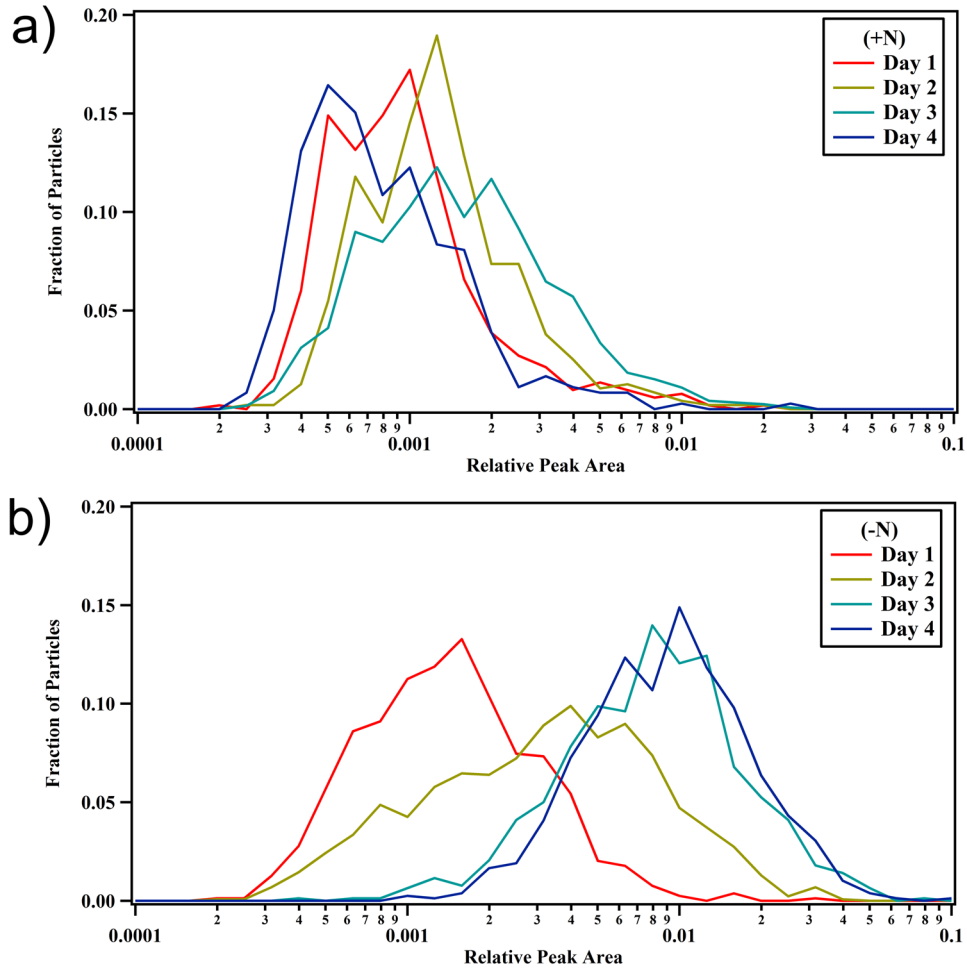

Figure 6. ATOFMS peak area distributions for m/z −794 of *Chlamydomonas reinhardtii* cells under nitrogen-replete (a) and nitrogen-limited (b) conditions.

fatty acid peak areas than in nitrogen-replete conditions. This is in agreement with other studies indicating increased TAG content in *Cr* cells with nitrogen-limitation.[40−44]

Average ATOFMS peak areas of thousands of single cells for the SQDG peak at m/z −794 for nitrogen-replete and nitrogen-limited conditions are shown in Figure 5b. Peak areas increase over time under nitrogen-limited conditions, consistent with an increase in 16:0 fatty acid content. In contrast, nitrogen-replete conditions remained similar for the course of the study. Comparisons of ATOFMS peak area measurements with other techniques such as GC/MS are difficult, as the two techniques utilize different methods for generating ions.[49,50] Nevertheless, the discrepancies between GC/MS and ATOFMS peak areas can partially be explained on the basis of instrument sensitivity.

Across all days, 30−40% of cells measured by ATOFMS had measurable peaks at m/z −794 in the nitrogen-replete condition. The low fraction containing m/z −794 could be due to being near the ATOFMS instrument sensitivity for this ion or from incomplete ablation of the cell arising from shot-to-shot laser variance. For nitrogen-limited samples, day 1 had a similar fraction of particles containing m/z −794, 52%, which increased to 70% by day 2 and to 100% by day 3. The major change in ATOFMS peak area occurred between days 2 and 3, when GC/MS peak areas ranged from 2.8 to 3.9 × 10^7. Assuming the ATOFMS sensitivity lies somewhere within this range of GC/MS peak areas, it is then reasonable to expect no change in ATOFMS peak area for the nitrogen-replete condition which never had GC/MS peak areas >2.0 × 10^7. Average m/z −794 peak area for trials 2 and 3 had similar trends to trial 1 (Figures S-11 and S-14)

Single Cell SQDG Profiles. The main goal in using the ATOFMS is to investigate metabolites at the single cell level. Single cell SQDG peak area histograms are shown in Figure 6 for nitrogen-replete and nitrogen-limited conditions. Under nitrogen-replete conditions, peak area distributions remain similar over every day of the experiment. Note the distributions of values are in part due to cell-to-cell heterogeneity and instrument variability. The same distribution is seen on day 1 for nitrogen-limited conditions, but as the experiment progresses, the distribution shifts toward higher peak areas consistent with the average peak areas shown in Figure 5b. On day 2, the single cell distribution broadens by 40% over any other day. This broadening extends beyond instrument variability and serves as an indicator of differences occurring at the single cell level. An average value of many cells, like those shown in Figure 5, would miss this feature entirely. The results suggest a lag of <1 day in the response of a subpopulation of cells to nutrient deprivation. The exact reasons for this will require further study. Thousands of cells were used to generate these distributions resulting in highly resolved peak area distributions, which are made possible by the unprecedented throughput of the ATOFMS for single cell analysis. The high

DOI: 10.1021/acs.analchem.5b02326
Anal. Chem. 2015, 87, 8039−8046

throughput allows one to statistically resolve differences in cell populations.[51]

CONCLUSIONS

We have demonstrated the application of a new technique utilizing an aerodynamic lens designed to allow larger particles or cells into an ATOFMS, allowing measurement of single cell mass spectra with unprecedented throughput. Cells were verified to be delivered intact after nebulization using a combination of sizing and imaging measurements, though some fragmentation of cells did occur. Both prokaryotic and eukaryotic microorganisms were sampled within the instrument, all of which generated complex mass spectra.

The microalgae *Chlamydomonas reinhardtii* was examined under nitrogen-replete and nitrogen-limited conditions. This represents the first reported time-resolved single cell mass spectral measurements of nutrient deprivation in green microalgae. Thousands of single cells were measured over a period of 4 days for both conditions. Comparison of ATOFMS mass spectra between the two conditions revealed an increase in the dipalmitic acid sulfolipid sulfoquinovosyldiacylglycerol (SQDG), a chloroplast membrane lipid, under nitrogen-limited conditions. "Bulk" measurements of SQDG by ATOFMS qualitatively agree with 16:0 fatty acid content measured by GC/MS. Single cell peak area distributions show the same biological information as "bulk" values, yet also show that subpopulations of cells have different SQDG levels when responding to nitrogen-limited conditions. This demonstrates the ability of the ATOFMS to measure metabolic differences in cells under environmental stress.

Future work will focus on improving the sensitivity of the ATOFMS toward other common lipids found in cells. Efforts to improve the quantitative nature of the mass spectra are also essential to future studies of single cell lipid content. The high vacuum of the instrument currently limits analysis to cells with high vacuum tolerance, such as those with a cell wall. Additional preparation techniques such as fixatives could be used to sample more fragile organisms reliably.

Currently, the ATOFMS has a maximum sampling rate of 50 Hz, significantly higher than most alternative single cell MS techniques but alternate desorption/ionization lasers with repetition rates up to kilohertz could be implemented to increase the throughput of the ATOFMS even further. The combination of simple sample preparation and high throughput lends itself to quick screening of metabolites or distinguishing and studying different cell populations in heterogeneous samples. Clustering techniques could be used to rapidly identify and differentiate single cells "on the fly". A high repetition laser would provide unique mechanistic insights into cellular processes in real-time.

ASSOCIATED CONTENT

Supporting Information

The Supporting Information is available free of charge on the ACS Publications website at DOI: 10.1021/acs.analchem.5b02326.

Supplemental discussion and Figures S-1−S-16 (PDF)

AUTHOR INFORMATION

Corresponding Author

*E-mail: kprather@ucsd.edu. Phone: 858-822-5312. Fax: 858-534-7042.

Present Addresses

[‖]J.F.C.: Oak Ridge National Laboratory, Organic and Biological Mass Spectrometry group, Oak Ridge, TN, 37932.

[⊥]N.G.S.: Division of Chemistry and Chemical Engineering, California Institute of Technology, 1200 E. California Blvd., Pasadena, CA 91125.

Notes

The authors declare no competing financial interest.

ACKNOWLEDGMENTS

Funding for this work was provided by NIH SBIR Phase II Contract No. HHSN26120100098C, DOE Grant DE-EE0003373, and NSF through the Center for Chemical Innovation program, Grant CHE1305427. The authors would like to thank Dr. Yongxuan Su for the collection of ESI MS/MS data and advice in interpretation of the mass spectra.

REFERENCES

(1) Wang, D. J.; Bodovitz, S. *Trends Biotechnol.* **2010**, *28*, 281−290.
(2) Heinemann, M.; Zenobi, R. *Curr. Opin. Biotechnol.* **2011**, *22*, 26−31.
(3) Amantonico, A.; Urban, P. L.; Zenobi, R. *Anal. Bioanal. Chem.* **2010**, *398*, 2493−2504.
(4) Zenobi, R. *Science* **2013**, *342*, 1201.
(5) Woods, L. A.; Ewing, A. G. *Anal. Bioanal. Chem.* **2003**, *376*, 281−283.
(6) Woods, L. A.; Roddy, T. P.; Ewing, A. G. *Electrophoresis* **2004**, *25*, 1181−1187.
(7) Huang, W. H.; Ai, F.; Wang, Z. L.; Cheng, J. K. *J. Chromatogr. B: Anal. Technol. Biomed. Life Sci.* **2008**, *866*, 104−122.
(8) Cohen, D.; Dickerson, J. A.; Whitmore, C. D.; Turner, E. H.; Palcic, M. M.; Hindsgaul, O.; Dovichi, N. J. *Annu. Rev. Anal. Chem.* **2008**, *1*, 165−190.
(9) Kennedy, R. T.; Oates, M. D.; Cooper, B. R.; Nickerson, B.; Jorgenson, J. W. *Science* **1989**, *246*, 57−63.
(10) Hu, S.; Michels, D. A.; Fazal, M. A.; Ratisoontorn, C.; Cunningham, M. L.; Dovichi, N. J. *Anal. Chem.* **2004**, *76*, 4044−4049.
(11) Krylov, S. N.; Zhang, Z. R.; Chan, N. W. C.; Arriaga, E.; Palcic, M. M.; Dovichi, N. J. *Cytometry* **1999**, *37*, 14−20.
(12) Krylov, S. N.; Arriaga, E. A.; Chan, N. W. C.; Dovichi, N. J.; Palcic, M. M. *Anal. Biochem.* **2000**, *283*, 133−135.
(13) Lapainis, T.; Rubakhin, S. S.; Sweedler, J. V. *Anal. Chem.* **2009**, *81*, 5858−5864.
(14) Fagerer, S. R.; Schmid, T.; Ibanez, A. J.; Pabst, M.; Steinhoff, R.; Jefimovs, K.; Urban, P. L.; Zenobi, R. *Analyst* **2013**, *138*, 6732−6736.
(15) Urban, P. L.; Schmid, T.; Amantonico, A.; Zenobi, R. *Anal. Chem.* **2011**, *83*, 1843−1849.
(16) Huang, B.; Wu, H. K.; Bhaya, D.; Grossman, A.; Granier, S.; Kobilka, B. K.; Zare, R. N. *Science* **2007**, *315*, 81−84.
(17) Shrestha, B.; Vertes, A. *Anal. Chem.* **2009**, *81*, 8265−8271.
(18) Tsuyama, N.; Mizuno, H.; Tokunaga, E.; Masujima, T. *Anal. Sci.* **2008**, *24*, 559−561.
(19) Mizuno, H.; Tsuyama, N.; Harada, T.; Masujima, T. *J. Mass Spectrom.* **2008**, *43*, 1692−1700.
(20) Tejedor, M. L.; Mizuno, H.; Tsuyama, N.; Harada, T.; Masujima, T. *Anal. Chem.* **2012**, *84*, 5221−5228.
(21) Amantonico, A.; Urban, P. L.; Fagerer, S. R.; Balabin, R. M.; Zenobi, R. *Anal. Chem.* **2010**, *82*, 7394−7400.
(22) Amantonico, A.; Oh, J. Y.; Sobek, J.; Heinemann, M.; Zenobi, R. *Angew. Chem., Int. Ed.* **2008**, *47*, 5382−5385.
(23) Lanni, E. J.; Rubakhin, S. S.; Sweedler, J. V. *J. Proteomics* **2012**, *75*, 5036−5051.
(24) Ibanez, A. J.; Fagerer, S. R.; Schmidt, A. M.; Urban, P. L.; Jefimovs, K.; Geiger, P.; Dechant, R.; Heinemann, M.; Zenobi, R. *Proc. Natl. Acad. Sci. U. S. A.* **2013**, *110*, 8790−8794.

DOI: 10.1021/acs.analchem.5b02326
Anal. Chem. 2015, 87, 8039−8046

(25) Urban, P. L.; Schmidt, A. M.; Fagerer, S. R.; Amantonico, A.; Ibanez, A.; Jefimovs, K.; Heinemann, M.; Zenobi, R. *Mol. BioSyst.* **2011**, *7*, 2837−2840.
(26) Trouillon, R.; Passarelli, M. K.; Wang, J.; Kurczy, M. E.; Ewing, A. G. *Anal. Chem.* **2013**, *85*, 522−542.
(27) Rubakhin, S. S.; Romanova, E. V.; Nemes, P.; Sweedler, J. V. *Nat. Methods* **2011**, *8*, S20−S29.
(28) Svatos, A. *Anal. Chem.* **2011**, *83*, 5037−5044.
(29) Schmid, A.; Kortmann, H.; Dittrich, P. S.; Blank, L. M. *Curr. Opin. Biotechnol.* **2010**, *21*, 12−20.
(30) Cannon, D. M., Jr.; Winograd, N.; Ewing, A. G. *Annu. Rev. Biophys. Biomol. Struct.* **2000**, *29*, 239−263.
(31) Moco, S.; Schneider, B.; Vervoort, J. *J. Proteome Res.* **2009**, *8*, 1694−1703.
(32) Urban, P. L.; Jefimovs, K.; Amantonico, A.; Fagerer, S. R.; Schmid, T.; Madler, S.; Puigmarti-Luis, J.; Goedecke, N.; Zenobi, R. *Lab Chip* **2010**, *10*, 3206−3209.
(33) Cahill, J. F.; Suski, K.; Seinfeld, J. H.; Zaveri, R. A.; Prather, K. A. *Atmos. Chem. Phys.* **2012**, *12*, 10989−11002.
(34) Kim, M.; Cahill, J. F.; Fei, H. H.; Prather, K. A.; Cohen, S. M. *J. Am. Chem. Soc.* **2012**, *134*, 18082−18088.
(35) Kim, M.; Cahill, J. F.; Su, Y. X.; Prather, K. A.; Cohen, S. M. *Chemical Science* **2012**, *3*, 126−130.
(36) Russell, S. C.; Czerwieniec, G.; Lebrilla, C.; Steele, P.; Riot, V.; Coffee, K.; Frank, M.; Gard, E. E. *Anal. Chem.* **2005**, *77*, 4734−4741.
(37) Pratt, K. A.; Mayer, J. E.; Holecek, J. C.; Moffet, R. C.; Sanchez, R. O.; Rebotier, T. P.; Furutani, H.; Gonin, M.; Fuhrer, K.; Su, Y. X.; Guazzotti, S.; Prather, K. A. *Anal. Chem.* **2009**, *81*, 1792−1800.
(38) Cahill, J. F.; Darlington, T. K.; Wang, X.; Mayer, J.; Spencer, M. T.; Holecek, J. C.; Reed, B. E.; Prather, K. A. *Aerosol Sci. Technol.* **2014**, *48*, 948−956.
(39) Allen, J. O. *YAADA Software Toolkit to Analyze Single-Particle Mass Spectral Data*, 2002; http://www.yaada.org.
(40) Korkhovoy, V. I.; Blume, Y. B. *Cytol. Genet.* **2013**, *47*, 349−358.
(41) Bolling, C.; Fiehn, O. *Plant Physiol.* **2005**, *139*, 1995−2005.
(42) Klok, A. J.; Martens, D. E.; Wijffels, R. H.; Lamers, P. P. *Bioresour. Technol.* **2013**, *134*, 233−243.
(43) Barreiro, A.; Hairston, N. G. *J. Plankton Res.* **2013**, *35*, 1339−1344.
(44) Hu, Q.; Sommerfeld, M.; Jarvis, E.; Ghirardi, M.; Posewitz, M.; Seibert, M.; Darzins, A. *Plant J.* **2008**, *54*, 621−639.
(45) Moellering, E.; Miller, R.; Benning, C. In *Lipids in Photosynthesis*; Wada, H., Murata, N., Eds.; Springer: Dordrecht, The Netherlands, 2010; Vol. *30*, pp 139−155.
(46) Siaut, M.; Cuiné, S.; Cagnon, C.; Fessler, B.; Nguyen, M.; Carrier, P.; Beyly, A.; Beisson, F.; Triantaphylidès, C.; Li-Beisson, Y.; Peltier, G. *BMC Biotechnol.* **2011**, *11*, 7−7.
(47) Sugimoto, K.; Sato, N.; Tsuzuki, M. *FEBS Lett.* **2007**, *581*, 4519−4522.
(48) Riekhof, W. R.; Ruckle, M. E.; Lydic, T. A.; Sears, B. B.; Benning, C. *Plant Physiol.* **2003**, *133*, 864−874.
(49) Qin, X. Y.; Bhave, P. V.; Prather, K. A. *Anal. Chem.* **2006**, *78*, 6169−6178.
(50) Gross, D. S.; Galli, M. E.; Silva, P. J.; Prather, K. A. *Anal. Chem.* **2000**, *72*, 416−422.
(51) Traller, J. C.; Hildebrand, M. *Algal Res.* **2013**, *2*, 244−252.

DOI: 10.1021/acs.analchem.5b02326
Anal. Chem. 2015, 87, 8039−8046